Published in final edited form as:
Photonics Lasers Med. 2013 November 1; 2(4): 287–303. doi:10.1515/plm-2013-0030.

Techniques for fluorescence detection of protoporphyrin IX in skin cancers associated with photodynamic therapy

Kishore R. Rollakanti,
Department of Chemical and Biomedical Engineering, Cleveland State University, 2121 Euclid Avenue, Cleveland, OH 44115, USA; and Department of Biomedical Engineering, Cleveland Clinic, 9500 Euclid Avenue, Cleveland, OH 44195, USA

Stephen C. Kanick,
Thayer School of Engineering, Dartmouth College, 14 Engineering Drive, Hanover, NH 03755, USA

Scott C. Davis,
Thayer School of Engineering, Dartmouth College, 14 Engineering Drive, Hanover, NH 03755, USA

Brian W. Pogue, and
Thayer School of Engineering, Dartmouth College, 14 Engineering Drive, Hanover, NH 03755, USA

Edward V. Maytin
Department of Chemical and Biomedical Engineering, Cleveland State University, 2121 Euclid Avenue, Cleveland, OH 44115, USA; Department of Biomedical Engineering, Cleveland Clinic, 9500 Euclid Avenue, Cleveland, OH 44195, USA; and Department of Dermatology, Cleveland Clinic, 9500 Euclid Avenue, Cleveland, OH 44195, USA

Edward V. Maytin: MAYTINE@ccf.org

Abstract

Photodynamic therapy (PDT) is a treatment modality that uses a specific photosensitizing agent, molecular oxygen, and light of a particular wavelength to kill cells targeted by the therapy. Topically administered aminolevulinic acid (ALA) is widely used to effectively treat cancerous and precancerous skin lesions, resulting in targeted tissue damage and little to no scarring. The targeting aspect of the treatment arises from the fact that ALA is preferentially converted into protoporphyrin IX (PpIX) in neoplastic cells. To monitor the amount of PpIX in tissues, techniques have been developed to measure PpIX-specific fluorescence, which provides information useful for monitoring the abundance and location of the photosensitizer before and during the illumination phase of PDT. This review summarizes the current state of these fluorescence detection techniques. Non-invasive devices are available for point measurements, or for wide-field optical imaging, to enable monitoring of PpIX in superficial tissues. To gain access to information at greater tissue depths, multi-modal techniques are being developed which

Correspondence to: Edward V. Maytin, MAYTINE@ccf.org.
Conflict of interest: The authors declare no conflict of interest.

combine fluorescent measurements with ultrasound or optical coherence tomography, or with microscopic techniques such as confocal or multiphoton approaches. The tools available at present, and newer devices under development, offer the promise of better enabling clinicians to inform and guide PDT treatment planning, thereby optimizing therapeutic outcomes for patients.

Keywords

protoporphyrin IX; fluorescence; photodynamic therapy; treatment planning

1 Introduction

Photodynamic Therapy (PDT) is a treatment technique in which cancerous tissues (solid tumors of the skin or other organs) are treated with a photosensitizing compound (photosensitizer, PS), followed by exposure to very intense, visible light [1]. The current availability of intense light sources, including a variety of lasers (LASER = light amplification by stimulated emission of radiation) [2, 3], generally insures that, for dermatological lesions, sufficient light intensity can be delivered during therapy. However, the other determinants for therapeutic success with PDT, namely, an adequate accumulation of the PS and supply of oxygen to all parts of the tumor, is less predictable and dynamically changing during treatment. PS accumulation is dependent both upon biochemistry and tumor biology and involves the uptake, synthesis, and degradation of the PS and/or its precursors. For understanding patient-specific variability in this latter aspect, a non-invasive way of monitoring PS accumulation in target tumors would be very desirable to help establish therapeutic parameters (PS dosing, light intensity and exposure time) associated with effective PDT therapy, and ideally, to use online information to tailor these parameters for each individual patient during PDT. This article reviews the prospects for non-invasive monitoring of PS to potentially serve as a guide to PDT, with a focus upon the use of aminolevulinic acid (ALA)-based PDT for the treatment of skin cancer. To establish the context for the article, we will begin with an introduction of principles involved in PDT, i.e., synthesis of protoporphyrin IX (PpIX), measurement of inducible PpIX fluorescence in tissue, and light-activated destruction of PpIX, followed by a discussion of past and current approaches for detecting PpIX through non-invasive fluorescence imaging.

1.1 Photodynamic therapy

1.1.1 General mechanisms of photodynamic therapy—The first generally recognized description of photodynamic killing of living cells using a photosensitizing agent was an observation by Oscar Raab in 1900 [4] that protozoa died when exposed to acridine orange and visible light. Subsequent research has shown that the three essential elements required for an effective phototherapeutic response are: (*i*) a PS, (*ii*) light of the correct wavelength to activate PS, and (*iii*) oxygen in the tissue [5]. When a PS (or PS precursor) is administered to patients (either topically or systemically, depending upon the particular agent), it is taken up by all cells and tissues. Yet PDT provides excellent tumor targeting due to two factors, namely (*i*) the selective accumulation (or production) of the PS in tumor cells as compared to normal tissue, and (*ii*) targeted illumination of the tumor tissue volume. When a PS absorbs light, the absorbed photon excites the PS to an energy-rich, excited state

(PS*), which then decays by a process called internal conversion. For molecules that are not photosensitizers, the energy of an absorbed photon is quickly converted to heat through efficient internal conversion, but for PS*, the internal conversion process is delayed by transition to a long-lived triplet-state. This gives the PS* more time to react with other molecules in its surroundings (Figure 1). In a Type-I reaction, PS* reacts directly with biomolecular substrates to produce free-radical ions, which then secondarily react with oxygen to produce highly reactive oxygenated species (e.g., superoxide radical anion). In a Type-II reaction, the energy in PS* is transferred to oxygen molecules in the local environment; i.e., molecular oxygen in its triplet ground state ($^3O_2$) is converted to singlet oxygen ($^1O_2$), a highly reactive and cytotoxic species [6, 7]. Subcellular damage that occurs from oxygenated products in the vicinity of the PS, leads to cell death and eventual tumor destruction [5, 8].

1.1.2 Unique features of photodynamic therapy, versus other cancer therapies —Traditional modalities for cancer treatment are surgery, ionizing radiation, and chemotherapy. However, the side effects of those treatments are significant and include the loss of healthy tissue, generation of additional cancers (radiation-induced mutations), and development of drug resistance, respectively. By comparison, PDT can be repeated multiple times, since it has very low carcinogenic potential, causing no damage to DNA [9]. In addition, skin tumors clear after PDT with little or no scarring [10]. In fact, PpIX-mediated PDT may actually have anti-scarring properties [11]. This is not true for all tissues, however. For example, scarring strictures can be a major problem after PDT of the esophagus [12].

1.1.3 Biochemistry and clinical applicability of PpIX-based PDT—In the early 1970s, the use of hemoglobin derivatives as PS for oncology was pioneered by Kessel, Dougherty and others, spawning the development of subsequent synthetic PS that are based generally upon a porphryin-like structure (historically reviewed in [13]). A number of such PS are currently in clinical use for treatment of cancers of internal organs, which requires the systemic administration of the PS and delivery of light into body cavities via an optical fiber. The use of PDT in general oncology is a large topic and outside the scope of this review; however, Anand et al. [14] gives a concise summary of current PDT regimens and medical disease indications. The current review will focus upon skin cancer and the most frequently used PDT techniques for skin cancer treatment. More clinical details about the status of PDT in dermatology can be found in the comprehensive review by MacCormack [10].

A desire to avoid systemic phototoxicity, which can sometimes be seen when using systemic PSs, was a driving force behind the development of alternative agents that can be topically applied to skin cancers and thereby affect only the area of interest. Toward this end, the work of Moan, Batlle, Kennedy, and Pottier (reviewed in [13]) established the principle of priming cells with an exogenous pro-drug (ALA) to induce the synthesis of an endogenous PS (PpIX). The idea here is that cancer cells can selectively accumulate PS through a process in which the PS is synthesized preferentially in the cancer cells; an idea that is central to the success of PpIX-mediated PDT. Thus, in the cellular heme biosynthetic pathway, δ-ALA leads to the formation of PpIX in the inter-membranous space of

mitochondria after a cascade of enzymatic reactions (Figure 2). Under normal physiological conditions, ferrochelatase catalyzes the insertion of iron into the PpIX to form heme, which regulates the synthesis of ALA via a negative feedback mechanism [15]. However, addition of exogenous ALA bypasses this feedback control and allows excess synthesis of PpIX within mitochondria. Production of PpIX is typically higher in tumors than in normal tissues because certain enzymes in the heme pathway are up- or down-regulated in the cancer cell, allowing PpIX to accumulate to significantly higher levels [16].

Modulating this biochemical process using adjuvant agents to elevate PpIX accumulation in non-responsive tumors is an active area of research. Recent studies in animal models have demonstrated increased PpIX levels resulting from pre-treatment of methotrexate (MTX), Vitamin D, or 5-Fluorouracil (5-FU) prior to ALA administration [14]. Coupling these differentiation approaches with real-time monitoring techniques could facilitate truly personalized PDT with greater efficacy, as discussed in later sections.

1.1.4 Physics of PpIX-fluorescence emission—The fluorescent properties of PpIX are related to its absorption characteristics. Figure 3 shows the PpIX absorption spectrum and emission spectrum, respectively, which together illustrate the Stokes shift (defined as the difference between the positions of the maximal band of the absorption and emission spectra, 405 nm and 635 nm, respectively). PpIX exhibits maximum light absorption (the Soret peak) at 405 nm and a much weaker absorption band at 635 nm. The latter can be used to excite PpIX while reducing interference from blood-borne hemoglobin (which has lower absorption at 635 nm). PpIX exhibits characteristic dual emission peaks at 635 nm and 705 nm; both of which can be measured readily *in vivo*.

The photochemical reactions that occur during PDT generate radical species that are not only cytotoxic to cellular components, but also react with and destroy the ground state PS. As a result, the available amount of ground state PS decreases as the reaction proceeds, resulting in a drop in the fluorescence intensity being measured; this process is termed photobleaching. Wilson et al. [17] proposed that this easily-observable quantity is an indirect metric of the therapeutic dose delivered during a PDT treatment.

1.2 Use of photosensitizers for fluorescence imaging

1.2.1 PpIX as a theranostic agent—PSs such as PpIX, in addition to their therapeutic potential, can function as fluorescent probes to assist in imaging of tumors. Thus, much interest has grown up around the use of PpIX (and other pre-formed PS) as “theranostic” agents, defined as molecular probes that have both therapeutic and diagnostic potential. The subject of PpIX as a photodiagnostic agent to identify and demarcate the margins of tumors is a very broad subject, and one that is too vast to be covered adequately in this review, which will instead focus on how the fluorescent properties of PpIX can be used to monitor changes during PDT therapy. The following sections discuss some issues regarding fluorescence monitoring during PpIX-based PDT.

1.2.2 Role of photobleaching versus singlet oxygen measurements in PpIX treatment monitoring—Photobleaching, as defined in section 1.1.4, is an indirect (or implicit) measure of the activation of PpIX and generation of oxygen radical species at the

treatment site. Direct monitoring of the reactive oxygen species generated during PDT is also possible, via sampling of singlet oxygen luminescence; however, the implementation of that approach is challenging due to the very low luminescence signals produced by singlet oxygen. Nonetheless, singlet oxygen during PDT has been measured using a variety of point-based systems and recently an imaging instrument [18–21]. In a recent example for interstitial treatments, Gemmell et al. [22] was successful in recording the $^1O_2$ luminescence at 1270 nm wavelength using a superconducting nanowire single-photon detector, which has promise for applicability *in vivo*. A detailed comparison of both singlet oxygen luminescence and PS photobleaching was recently reviewed by Wilson and Patterson [23].

Photobleaching has been investigated in many studies as a means to monitoring the progress of PpIX treatments in skin. A compact fluorescence spectrometer was developed by Nadeau et al. [24] in 2004 to monitor the photobleaching of ALA-induced PpIX in the skin of healthy volunteers. This spectrometer incorporated 405 nm and 633 nm excitation sources into a fiber optic sampling system, which provided an estimate of background (autofluorescence), PpIX, and other photoproducts. The instrument allowed quantification of various photoproducts and showed that blue light causes more rapid photobleaching than red light. Moan et al. [25] also studied the effects of light exposure on PpIX degradation and PpIX reappearance at 420 nm and 632 nm in mice. They found that the PpIX reappearance rate is faster if the skin is exposed to 420 nm light after 0.5 h of methyl-ALA (MAL) application. In another study using fluorescence spectroscopy measurements of PpIX, it was suggested that photosensitivity can be significantly reduced with the cream formulation containing PpIX precursors with ferrous or cobalt ions [26].

1.2.3 Factors complicating fluorescence detection of PpIX in tissue—The influence of tissue optics on fluorescence measurements were comprehensively reviewed by Wagnières et al. [27]. Thus, important properties that influence fluorescence measurements in tissues are: (*i*) attenuation of light in the tissue; (*ii*) presence of endogenous fluorophores which cause autofluorescence; (*iii*) absorption; (*iv*) scattering; and (*v*) reflection of light. Many traditional (pre-formed) PSs have short excitation wavelengths, usually in the range of ultraviolet (UV)-blue, and at these wavelengths most of the light is attenuated in the superficial layers, making fluorescence diagnosis with short-wavelength excitation impossible for deeply seated tumors. This can potentially be circumvented using longer excitation wavelengths that penetrate more deeply into tissue. For example, 635 nm red laser light can excite PpIX at greater depths than is possible with 400 nm light, and the use of even longer, near-infrared (NIR) wavelengths (using two-photon excitation) may allow detection of deeper-seated tumors [28, 29] (see also section 3.3).

An understanding of the physics of light–tissue interaction requires sophisticated experimental and computer modeling. As excitation light and the emitted light pass through the tissue, the scattering and absorption properties at excitation and emission wavelengths can strongly influence the fluorescence emission intensity within the tissue, resulting in wide variations in spectral shape of the light that emerges [30–32]. There are a plethora of approaches to correct for the distortive influences of optical properties on fluorescence measurements (reviewed by Bradley and Thorniley [33]). To control and understand these phenomena, tissue phantoms (such as translucent gels which simulate the optical properties

of tissues) can be used to model light–tissue interactions [34]. More complex tissue models, such as tumors implanted in mice or rats, can also be used to study the fluorescence diagnostic potential and PDT therapeutic efficacy of PpIX, and to develop approaches to correct for the distortive effects, either through empirical or model-based correction algorithms. An example of a quantitative approach to PpIX measurement is given by Brian Wilson's group [35], which presented a method for tissue fluorescence quantification *in situ* using a handheld fiber optic probe that measures both the fluorescence and diffuse reflectance spectra to decouple the fluorescence spectrum from distorting effects of tissue optical absorption and scattering. More generally, the correction approaches are device- and probe specific, as will become clear in the subsequent sections.

2 Detection of PpIX in the skin using surface measurements

On the basis of the kinds of optical instrumentation used for illumination and detection, studies on the photodetection of PpIX in the skin can be broadly classified into two categories, namely (1) fiber optic probe/ point spectrofluorometry, and (2) wide-field camera-based imaging. Each of these approaches has its own pros and cons. In point spectrofluorometry, the excitation light probe is placed in direct contact with the tissue and the emitted signal is measured within a restricted area, typically 50–1000 μm in diameter [36]. This sampling approach has several advantages, namely: (*i*) probe geometry measurements are generally more sensitive than wide-field techniques; (*ii*) facilitate easy implementation of spectral or time-domain detection; and (*iii*) the localized signal is not 'washed out' amongst the noise of heterogeneities throughout the tissue. However the signal is only representative of a small sampled volume, and cannot characterize spatial variations in PS fluorescence either within a large lesion, or between multiple lesions. For the latter purpose, a wide-field imaging approach is advantageous. However, standard wide-field imaging techniques sample a diffuse signal, with each pixel in the image collecting light that has travelled a range of paths and traversed a range of volumes within the tissue, yielding a volume-averaged signal. Moreover, the likelihood of collecting photons from non-targeted structures within the tissues is higher in the wide-field imaging approach, possibly leading to inaccurate results. Therefore, special care must be taken to obtain accurate spatial maps of the fluorophore from wide-field imaging-based devices.

Regarding drawbacks, one potential problem with point measurements is that the probe can exert pressure-related effects, introducing variation into the fluorescence measurements. This was nicely shown in a study by Lim et al. [37], in which significant changes in measured fluorescence were recorded as the pressure of the probe tip against the skin was increased; these deviations correlated strongly with compression of blood flow, and less strongly with changes of autofluorescence emanating from collagen. With wide-field camera approaches, the relatively low collection efficiency of the detector (as compared to point probes) may restrict image quality [38].

As a final comment, a more accurate approach is to use spectrally-resolved fluorescence collection at multiple wavelengths, which allows for decoupling of multiple sources of fluorescence within the tissue (including PS, photoproducts of the PS generated during treatment, and tissue autofluorescence), and this is most often done using point probe

measurements. In the following sections, specific examples in which fluorescence was measured either using a point probe, or a wide-field camera technique, are described to illustrate the types of information that can be obtained to help inform PDT treatment of skin cancer.

2.1 Fiber optic probe/ point measurements of PpIX

A point monitoring system was used by Wang et al. [39] to investigate the pharmacokinetics of PpIX accumulation in skin tumors (basal cell carcinomas, BCC; and T-cell lymphomas) and normal skin, at 4–6 h after applying non-fluorescent 20% ALA topically. Laser-induced excitation (405 nm) was used, and the emitted fluorescence was collected through the same quartz fiber and sent to a linear array detector to monitor both PpIX specific fluorescence (635 nm and 705 nm) and tissue autofluorescence (at 490 nm). At 4 and 6 h, tumors showed a marked increase in the fluorescence intensity at 635 nm and 705 nm relative to the pre-ALA baseline, and after correcting for autofluorescent background, the fluorescence intensity at 635 nm showed a high tumor-to-normal skin ratio, ranging from 9:1 to 15:1. A similar kind of study was done by Johansson et al. [40] to investigate the kinetics and dose-dependence of ALA-induced PpIX accumulation in different organs and tissue types in rats after intravenous administration of ALA. Fluorescence spectra from tumors and normal surrounding tissue were obtained using an optical fiber-based fluorosensor at 405 nm excitation wavelength. Using the recorded fluorescence spectra and correcting for autofluorescence, they observed that a maximum PpIX build-up in tumors was achieved within 1 h after ALA administration, as compared to the surrounding muscle, which is in harmony with other reports on intravenously (i.v.) injected ALA [41]. However, the distribution pattern for i.v. ALA in this study indicates a high PpIX level in the gastrointestinal organs, up to 10 times more than in tumors, which indirectly suggests that 1 h may not be the optimal time for observing high selectivity of PpIX in tumor. In another study, Rhodes et al. [42] used iontophoresis (application of electrical charge) to drive ALA into the skin over a time interval of seconds to minutes and measured the PpIX fluorescence using a fiber optic point source. Excitation light from a xenon arc lamp was focused through a monochromator and a bifurcated fiber optic cable to deliver 410 nm light to the skin; the fluorescence emission was then passed through another monochromator to detect the characteristic emission peaks at 635 and 704 nm.

Other studies to guide the development of PDT are those designed to determine the optimal formulation of ALA or ALA esters to use for photosensitization; many of these studies have used point probe measurements. The potential clinical advantage of using ALA esters was determined by observing the PpIX fluorescence non-invasively using point spectroscopy systems in both normal skin [43] and skin carcinomas [44, 45]. To seek improved topical drug delivery of ALA and its esters, Bender et al. [46] measured PpIX skin fluorescence after topical administration of MAL in lipid cubic phases (highly ordered self-assembly systems on a nanometer level) and found that some of the cubic phases imparted faster PpIX-forming ability than standard ointment formulation. Donnelly et al. [47] used point fluorescence measurements to compare the PpIX-forming ability of MAL contained in pressure sensitive adhesives with that of standard cream formulations, and showed higher production of PpIX with the patches.

Relatively few studies have examined the kinetics of PpIX synthesis in human skin. Using *in vivo* surface-detection fluorescence spectroscopy, Golub et al. [48] studied the accumulation and clearance of ALA-induced PpIX in patients with actinic keratoses (AK) and BCC, and showed that thick lesions have longer PpIX retention times than do thinner ones. A more difficult question is whether the amount of PpIX production in neoplastic lesions can predict successful clinical outcome. In a clinical study using a fluorescence point dosimeter, Warren et al. [49] asked whether PpIX-mediated fluorescence measurements are predictive of biological responses to ALA-PDT in squamous precancers (AK) in 20 patients. Excitation laser light of 405 nm wavelength was launched down a single 100-μm-diameter quartz optical fiber to the skin (Figure 4A), and the fluorescent light induced was collected by seven optical fibers surrounding the excitation fiber (Figure 4B), for measurement by a photodetector. Serial measurements taken every 30 min after ALA application revealed a linear rate of accumulation in all patients, with statistically significant PpIX levels reached in nearly 100% of patients by 2 h and thereby justifying the use of short-contact PDT in the clinic [49]. Moreover, the PpIX fluorescence amplitude was correlated with biological response, as measured by erythema within lesions (Figure 4C, D).

2.2 Wide-field camera-based imaging of PpIX

The fluorescence properties of PpIX can also be used to visualize the entire area of skin under investigation, which can be an advantage in some clinical studies. Fluorescence emitted by PpIX can aid in preclinical studies that follow the accumulation and dissipation of PS non-invasively [50–52]. Early imaging devices, such as the image-intensified camera introduced in 1979 by Profio et al. [53], did not have the capacity to image white light and fluorescence simultaneously, a drawback because the white light image is helpful for facilitating anatomic localization of the tumor. Later optical imaging systems, using liquid nitrogen cooled charge-coupled device (CCD) cameras, managed to circumvent this problem [54]. Recently, Tyrrell et al. [55] studied the accumulation and dissipation of PpIX in BCC during MAL-PDT using a commercially available, non-invasive fluorescence imaging system from Dyaderm, Biocam®. Using this system, they were able to quantify the level of MAL-induced PpIX in BCC tumors at different time points of interest, and concluded that lesions undergoing a second PDT treatment accumulate and dissipate less PpIX than during their first treatment. A blinded study on 30 skin cancer patients by van der Beek et al. [56] showed that PpIX photodiagnosis (with implications for detecting changes in PpIX in target lesions) is more efficient if PpIX fluorescence is combined with an analysis of autofluorescence, than if PpIX fluorescence is evaluated alone.

Although CCD camera systems can facilitate the localization of tumors, restriction to a single wavelength is a serious limitation that precludes spectrally decoupling different sources of fluorescence. Various attempts have been made to incorporate fluorescence measurements at several wavelengths to better compensate for autofluorescence and background optical properties. Approaches tried include sequential imaging at different excitation and emission wavelengths [57, 58], and time-gated imaging [59]. Andersson-Engel et al. [60] designed a multi-color fluorescence imaging system to record four fluorescent images in different wavelength bands, i.e., 635 nm (PpIX fluorescence), 470 and 600 nm autofluorescence, and 670 nm (photobleached products emission at 670 nm from

normal and malignant tissues). They used this multi-color imaging system to construct a false color-coded image to use as a tool for delineation of malignant tumors, and for monitoring PS levels during PDT. Other groups took similar approaches, constructing false-color maps from fluorescent images recorded at two or three wavelengths, which could be used to try to monitor PpIX levels during PDT [61, 62].

The above fluorescence imaging techniques return spatial maps of PpIX fluorescence emission, which may be influenced by either variations in the quantity of PpIX or by variations in the background tissue optical properties. Approaches that attempt to quantify PpIX in tissue must properly decouple these effects. Spatial frequency domain imaging (SFDI) is one such approach, which uses an empirical model to interpret remission in response to illumination with patterns of selected spatial frequencies, and returns spatial maps of estimated scattering and absorption properties within the sampled medium [63]. The distributions of optical properties are used to inform a correction of the sampled raw fluorescence to estimate a quantitative metric of PpIX concentration *in vivo* [64]. The SFDI approach has been used to quantify PpIX in BCC and squamous cell carcinomas (SCCs) [65], with *in vivo* estimates highly correlated with *ex vivo* analysis techniques.

More technologically advanced imaging using hyperspectral approaches have been proposed to return increased resolution, but which may or may not have direct extensibility to skin-based PDT. For example, Valdés et al. [66] described a dual-band normalization technique for *in vivo* quantification of PpIX during brain tumor resection; the PpIX fluorescence signal is corrected with reflectance data recorded and integrated within only two narrow wavelength intervals, a very simple method that could be applicable to wide-field applications in quantitative fluorescence imaging and dosimetry during PDT. Another device, reported by Lue et al. [67], is a portable, optical fiber probe-based, spectroscopic tissue scanner designed for intraoperative diagnostic imaging of surgical margins. The scanner combines both diffuse reflectance spectroscopy and intrinsic fluorescence spectroscopy, and has hyperspectral imaging capability that allows the device to provide high spectral resolution (2 nm), and high spatial resolution (0.25 mm) over a wide field of view (10 cm × 10 cm).

A full consideration of the current state-of-the-art in high resolution molecular imaging technologies is incomplete without mention of novel microscopy techniques. Structured illumination microscopy (SIM) is one such tool that has been used to study the characteristics of fluorescent molecules both *ex vivo* and *in vivo*. Rossberger et al. [68] demonstrated that SIM allows much more differentiated analysis of fluorochromes. They achieved a two-fold increase in resolution compared with standard wide-field microscopy and higher resolving power than confocal and multiphoton microscopy. Using complementary techniques like random intensity illumination and rotating view acquisition in combination with SIM, better depth information and increased reconstruction quality has been achieved in human and animal subjects [69, 70].

3 Approaches for measuring PpIX beneath the surface of the skin

A major concern in measuring PpIX fluorescence is an inability to quantify PpIX levels in thick skin carcinomas and deeply-seated tumors. Treatment failures are almost certainly due to unequal production of PpIX in all regions of target tumors, and several new combination PDT protocols, including differentiation therapy with MTX or vitamin D, are showing promise for enhancing the production of PpIX in subcutaneous tumors prior to PDT when examined by biopsy and histology (reviewed in [14]). However, *in vivo* monitoring of PpIX during these new combination protocols would be very desirable, and for this better tools are needed for monitoring at depth. Surface probe-based approaches and camera-based wide-field imaging, described in the previous sections, are not ideal because they cannot interrogate fluorescence at different depths within the lesion. A tomographic approach to collecting fluorescence light would seem a logical way to address this problem, but in fact, scattering and diffusion of light within tissues represents a major barrier to obtaining high-resolution two dimensional (2-D) fluorescent images. A potential, practical approach is to rely on a second technique, such as ultrasound (US) or optical coherent tomography (OCT), to provide high-resolution spatial information and to co-register this spatial image with the relatively poorly-defined image obtained using 2-D fluorescence tomography. Some co-registration approaches, using either US or OCT, are described below.

3.1 Ultrasound imaging combined with fluorescence imaging

Zhu et al. [71] in 2001 successfully coupled US and NIR imaging to overcome the deficiencies inherent in each of these imaging techniques. US has good image resolution capacity, but is not accurate in detecting cancer due to the overlapping characteristics of benign and malignant lesions. In contrast, NIR imaging of fluorescence can provide high specificity in detecting cancers (due to the tumor-selective nature of PpIX production within tumors), but suffers from poor resolution due to the diffusion of NIR light. With a hybrid imaging system, target depth information was more accurate and reconstruction speed was much faster [71]. High frequency ultrasound (HFUS) can also be used in dermatology as a non-invasive tool for monitoring the therapeutic efficacy of different drugs, and also to assess skin diseases [72]. To study dynamic changes in concentration of PpIX and its distribution in tissues, Gruber et al. [34] developed a hybrid fluorescence tomography system. This device (see Figure 5) combined a HFUS system with a multi-channel spectrometer-based fluorescence tomography system. In this hybrid arrangement, anatomical information from the US system is combined with the optical data to quantify PpIX activity in sub-surface lesions. Source and detector fibers were arranged in a linear, alternating fashion, immediately adjacent to the US probe. Using this system, co-registration of fluorescence signals and the HFUS image was validated in gel phantom studies. Studies *in vivo* demonstrated multimodal recovery of PpIX in subcutaneous A431 tumors. Interestingly, skin overlying the tumors showed more fluorescence than the tumors themselves, a finding validated using *ex-vivo* fluorescence scanning of these tissues. While still in development, this system represents a promising attempt to analyze variably-sized tumors which are present at different depths, and to evaluate the PpIX concentrations within them. The Dartmouth group recently released a paper describing updates to this system, which includes spectroscopic decoupling of fluorescence signals (autofluorescence, PpIX,

photoproducts), and the use of bulk optical properties determined from white light spectroscopy [73].

The success of HFUS when combined with 2-D fluorescence will ultimately depend on the usefulness of HFUS itself for delineating skin cancers. Desai et al. [74] and Crisan et al. [75] evaluated HFUS to adequately demarcate BCC tumors and tumoral thickness respectively. Of the 50 BCCs scanned by Desai et al. [74] using HFUS, 45 showed similar clinical confidence in margin assessment suggesting that ultrasonography may be a sensitive screening test if clinical or histologic diagnosis is uncertain. In their study involving BCC, superficial spreading melanoma and nodular melanoma subjects, Crisan et al. [75] identified a strong correlation between the ultrasonographic and the histological index values. In addition, they were successful in elaborating the reliability of HFUS as a tool for the non-invasive assessment of tumor thickness.

3.2 Optical coherence tomography combined with 2-D fluorescence tomography

OCT is the second technique discussed in this section, which has the potential to provide spatial co-registration with the relatively poorly-defined images of 2-D fluorescence tomography. First demonstrated in 1991, OCT has been recognized as a promising tool for diagnosing different pathological conditions like BCC, AK and SCC [76]. It offers high resolution cross-sectional tomographic images of the skin by measuring back-scattered and reflected light [77]. OCT is more accurate and less biased than HFUS in measuring the tumor thickness of AK and BCC which are <2mm deep [78]. However, relatively slow imaging speeds and a limited penetration depth have restricted the use of OCT for imaging large tissue volumes. Yun et al. [79] demonstrated that spectral-domain OCT (SD-OCT) can be used to achieve a higher image acquisition rate (38 fps), imaging depth (2 mm), and signal-to-noise ratio than is possible with time-domain OCT. Such frequency-domain OCT systems can be integrated with fluorescence subsurface tomography to locate fluorescent regions and to allow quantification of fluorescence with high speed and sensitivity over a depth range of 2 mm [80–82].

Boone at al. [83] recently introduced high-definition OCT (HD-OCT) based upon a modification of conventional OCT. This imaging tool has enabled them to visualize individual cells up to a depth of 570 μm with micrometer resolution in both horizontal (en-face) and vertical (slice) directions. Instead of a single pin diode, HD-OCT utilizes a 2-D infrared imaging array which allows the focal plane to be moved continuously through the sample, providing a high lateral and axial resolution at all depths, a resolution that allowed Boone et al. [83] to diagnose BCC and its subtypes non-invasively. Maier et al. [84] also used HD-OCT to investigate 22 BCC tumors and found that some of the features, such nests of basaloid tumor cells and cellular structures with lobules and buds, can be clearly visualized in the en-face imaging mode of HD-OCT.

Fluorescence confocal laser scanning microscopy (CLSM) is another novel technique that allows one to potentially diagnose nonmelanoma skin cancers by detecting fluorophores at different cell layers [85, 86]. The basic principle of confocal microscopy is to obtain images of higher optical resolution than that of conventional wide field microscopes by using point illumination and a pin hole. In confocal laser-scanning microscopy, a coherent laser light

source is used to excite the fluorophore molecules within a particular focal volume of the tissue. The fluorescence emitted from out-of-focus regions is blocked by the small pinhole in the detection aperture, thus resulting in sharp, high-resolution images at a particular depth. This focal plane can be shifted to deeper layers of tissue, enabling one to visualize fluorophores at various depths within the sample [87]. Fluorescent dyes can be used to detect the morphological characteristics of diseased skin (BCC, AKs) and can also be applied for the non-invasive monitoring of the lesional skin's response to therapy [88]. De Rosa et al. [89] used CLSM to determine the ability of dimethylsulphoxide and ethylenediamine-tetraacetic acid disodium salt to enhance the accumulation of ALA-induced PpIX in hairless mouse skin. The intensity of red fluorescence in the confocal microscopic images appeared to correlate with the results of independent PpIX quantification experiments.

3.3 Multiphoton tomography and fluorescence lifetime imaging

Multiphoton tomography (MPT) is the most recent imaging technology that facilitates deep imaging in biological tissues at very high resolution. In conventional confocal microscopy, fluorophores are excited by a single UV or visible photon, whereas in MPT imaging technology, fluorophores are excited by absorption of two (or more) photons of much longer wavelength, usually in the NIR spectrum. An individual NIR photon has insufficient energy to excite the fluorophore, but simultaneous absorption of two photons (upon addition of their interaction energies) elevates the fluorphore's electrons to an excited state (see Figure 6). The distinct advantage of the long wavelength photons is their ability to penetrate quite far into tissue, thus facilitating deep imaging [90–93].

Fluorescence lifetime imaging microscopy (FLIM) is an additional non-invasive imaging technique to study endogenous fluorescent molecules and their environment by using the decay rate of the fluorescence emission [94, 95]. The FLIM analysis produces pseudo color images in which the color scale encodes the fluorescence lifetime, and white image brightness encodes the fluorescence intensity. Thus, FLIM is useful to study the localization of proteins and other fluorescent molecules in their native environment. A combination of MPT and FLIM was shown to be useful for the study of fluorescent properties of normal skin [94] and also to characterize skin layer specificity [96]. Seidenari et al. [97] studied the specificity and sensitivity of MPT-FLIM for diagnosing BCC and specifying tumor margins; they identified several morphological and numerical descriptors for differentiating BCC from other skin lesions, and achieved extremely high specificity.

The possibility that MPT-FLIM might be able to take advantage of the fluorescence from ALA-induced PpIX is an attractive idea, since PpIX is a well-characterized fluorophore for imaging of human skin lesions. To date, most studies using PpIX fluorescence for MPT-FLIM imaging are limited to cell cultures [98, 99] and solutions [100]. Riemann et al. [101] used MPT on skin biopsies to study the biosynthesis of PpIX and also to evaluate the therapy. Cicchi et al. [102] demonstrated enhanced tumor contrast and depth of imaging by using MAL-induced PpIX as the contrast agent, and two-photon excitation (TPE) in combination with FLIM as the imaging technique. A similar study by Kantelhardt et al. [103] to identify gliomas achieved high contrast images of the glioma architecture that were

easily discriminated from normal brain tissue, by detecting ALA-induced PpIX fluorescence with multiphoton microscopy. A few other studies report the use of multiphoton excitation for PpIX detection [104], but offer no detailed spectral information.

In all the previous studies using TPE, the desired PpIX signal tended to be overshadowed by autofluorescent background. Kantere et al. [105] demonstrated that this background signal can be overcome by exciting the PpIX at a wavelength that gives rise to one-photon anti-Stokes fluorescence. They championed the use of anti-Stokes excitation at 710 nm wavelength, because the likelihood for one-photon anti-Stokes excitation is increased and the resulting PpIX emission is significantly higher than the autofluorescence, making the signal from ALA-induced PpIX easy to discern. Their system requires a trade-off between higher signal strength and lower resolution of the PpIX; thus, the resolution of anti-Stokes excited PpIX is not the same as in pure TPE, but the PpIX distribution in tissues can be more easily discerned. Their detailed spectral investigation also confirmed that PpIX emission from intact skin could only be obtained using 710 nm excitation, and cellular morphology could be visualized if combined with TPE of autofluorescence [105].

4 Planning and monitoring of PDT administration

Having described the various types of optical measurements that are available to measure fluorescence, the most challenging aspect for ongoing and future research will be to determine how these techniques might be used to tailor the PDT treatment regimen to obtain optimal clinical outcomes. One question is how fluorescence measurements can be used to inform patient-specific dosing (optimal ALA dose and light delivery) in the preplanning stages, prior to PDT. The need is great, because skin cancer response rates after PDT are extremely variable and it is currently impossible to predict which patients will respond favorably. As an example of such variability, large clinical trials show that overall response rates for SCC precancers (AKs) are only in the 60–80% range, with wide variability observed between patients [106, 107]. If rapid and accurate PpIX dosimetric measurements could be routinely obtained just prior to PDT light treatment, then the PpIX results might be used to tailor future therapy sessions for patients who failed to clinically respond. A particularly exciting possibility is that the PpIX dosimetric measurments could determine which patients might benefit from the application of adjuvant compounds, such as MTX and 5-FU, to enhance PpIX accumulation prior to PDT [14]. Another question is whether fluorescence techniques can assess one or more parameters measured at the end of treatment (e.g. photobleaching) to predict the long-term clinical outcome, the need for additional treatment(s), and necessary modifications to the regimen to be used in subsequent treatment sessions. A third question, clearly the most futuristic, is whether fluorescent measurement techniques can be used to monitor PpIX utilization (degradation rates) on an ongoing basis during the illumination phase, to permit adjustment of the light fluence rates in real time and thereby achieve an optimized light dose.

Overall, it must be emphasized that fluorescence monitoring for PDT of skin cancer is a field still in its infancy. However, a few studies which offer early indications of the power of fluorescence dosimetry to rationally tailor PDT regimens will be mentioned. In work by Tyrrell et al. [108] in the U.K., in which fluorescent measurements of PpIX in human skin

cancer patients undergoing MAL-based PDT were taken pre- and post-PDT, it was found that changes in PpIX levels during therapy (photobleaching), was a better predictor of clinical outcome (tumor clearance) than was the initial level of PpIX. Thus, for purposes of adjusting the light delivery, the wide lesion-to-lesion variability in PpIX levels may make pre-treatment measurements less valuable as an indicator of the potential for therapeutic dose, and necessitate instead ongoing measurements of PpIX degradation. Another set of studies, performed by the group of D. Robinson and co investigators in the Netherlands [109–112], illustrates the potential influence of the illumination scheme upon PpIX treatment efficacy. Through an elegant series of preclinical and clinical studies, this group showed that fractionating the administration of the therapeutic light dose significantly improves the clinical response of BCC to ALA-mediated PDT using red light. However, the mechanism remains obscure. Fluorescence measurements using limited technology demonstrated a non-homogenous distribution of PpIX in BCC tumors [111], and they also showed that significant PpIX accumulation occurs not only in tumor cells but in peritumoral blood vessels, thus implicating a role for vascular endothelial cells in the therapeutic response [109]. Clearly, a sensitive method to measure PpIX in these deep anatomic locations would be a valuable tool to dissect the mechanisms and optimize the therapeutic responses of skin tumors to PDT.

5 Conclusion

In this review, we began by establishing the importance of ALA-based PDT as a non-scarring treatment modality for skin cancer, but also pointed out that the promise of PDT is still hampered by the large variability in the accumulation levels of target protoporphyrin (PpIX) between different lesions and from patient-to-patient. Given this problem, the need to develop real-time, non-invasive techniques to detect and monitor PpIX levels within target lesions, so as to properly alter the delivered PDT dose and achieve the best therapeutic outcome, represents a critical goal. Porphyrin-derived fluorescence has great promise for non-invasively detecting PpIX in lesions, and this review discussed various imaging technologies to measure PpIX fluorescence, including probe-based point measurements and CCD camera-based wide-field imaging. We also described the use of tomographic fluorescence measurements as a co-modality with US, CLSM, MPT, and other techniques to provide increased resolution, specificity/accuracy, and sensitivity to the PpIX measurements in malignant skin lesions. Many of these new, research-based techniques have the potential to become clinically available for non-invasive treatment planning and on-line monitoring of PpIX levels. However, much work remains to be done to fulfill the goal of developing clinically viable systems that can facilitate treatment planning and on-line dosimetry in real time. Meeting this challenge will be difficult, requiring an interdisciplinary approach that involves physics, biology, chemistry and engineering. However, the result could be a much better therapeutic outcome for our patients.

Acknowledgments

All of the authors of this review received support from Program Project grant CA084203 from the National Cancer Institute, National Institutes of Health, USA.

References

1. Hasan, T.; Ortel, B.; Solban, N.; Pogue, B. Photodynamic therapy of cancer. In: Kufe, DW.; Bast, RC.; Hait, WN.; Hong, WK.; Pollock, R.; Weichselbaum, RR.; Gansler, T.; Holland, JF.; Frei, E., III, editors. Cancer Medicine. 7. Hamilton (Ontario, Canada): BC Decker, Inc; 2006. p. 537-48.
2. Goldman, L., editor. The biomedical laser. New York: Springer-Verlag; 1981.
3. Katzir, A. Lasers and optical fibers in medicine. San Diego: Academic Press; 1993.
4. Raab O. Über die Wirkung fluorescierender Stoffe auf Infusoria. Z Biol. 1900; 39:524–46.
5. MacDonald IJ, Dougherty TJ. Basic principles of photodynamic therapy. J Porphyrins Phathalocyanines. 2001; 5(2):105–29.
6. Moan J, Sommer S. Oxygen dependence of the photosensitizing effect of hematoporphyrin derivative in NHIK 3025 cells. Cancer Res. 1985; 45(4):1608–10. [PubMed: 3978628]
7. Henderson BW, Miller AC. Effects of scavengers of reactive oxygen and radical species on cell survival following photodynamic treatment in vitro: comparison to ionizing radiation. Radiat Res. 1986; 108(2):196–205. [PubMed: 3097749]
8. Foote CS. Mechanisms of photooxygenation. Prog Clin Biol Res. 1984; 170:3–18. [PubMed: 6531365]
9. Halkiotis K, Yova D, Pantelias G. In vitro evaluation of the genotoxic and clastogenic potential of photodynamic therapy. Mutagenesis. 1999; 14(2):193–8. [PubMed: 10229921]
10. MacCormack MA. Photodynamic therapy. Adv Dermatol. 2006; 22:219–58. [PubMed: 17249304]
11. Campbell SM, Tyrrell J, Marshall R, Curnow A. Effect of MAL-photodynamic therapy on hypertrophic scarring. Photodiagnosis Photodyn Ther. 2010; 7(3):183–8. [PubMed: 20728843]
12. Dunn JM, Mackenzie GD, Banks MR, Mosse CA, Haidry R, Green S, Thorpe S, Rodriguez-Justo M, Winstanley A, Novelli MR, Bown SG, Lovat LB. A randomised controlled trial of ALA vs. Photofrin photodynamic therapy for high-grade dysplasia arising in Barrett's oesophagus. Lasers Med Sci. 2013; 28(3):707–15. [PubMed: 22699800]
13. Juzeniene A, Peng Q, Moan J. Milestones in the development of photodynamic therapy and fluorescence diagnosis. Photochem Photobiol Sci. 2007; 6(12):1234–45. [PubMed: 18046478]
14. Anand S, Ortel BJ, Pereira SP, Hasan T, Maytin EV. Biomodulatory approaches to photodynamic therapy for solid tumors. Cancer Lett. 2012; 326(1):8–16. [PubMed: 22842096]
15. Berlin NI, Neuberger A, Scott JJ. The metabolism of delta-aminolaevulic acid. 1. Normal pathways, studied with the aid of 15N. Biochem J. 1956; 64(1):80–90. [PubMed: 13363809]
16. Kennedy JC, Pottier RH. Endogenous protoporphyrin IX, a clinically useful photosensitizer for photodynamic therapy. J Photochem Photobiol B. 1992; 14(4):275–92. [PubMed: 1403373]
17. Wilson BC, Patterson MS, Lilge L. Implicit and explicit dosimetry in photodynamic therapy: a new paradigm. Lasers Med Sci. 1997; 12(3):182–99. [PubMed: 20803326]
18. Patterson MS, Wilson BC, Graff R. In vivo tests of the concept of photodynamic threshold dose in normal rat liver photosensitized by aluminum chlorosulphonated phthalocyanine. Photochem Photobiol. 1990; 51(3):343–9. [PubMed: 2356229]
19. Niedre M, Patterson MS, Wilson BC. Direct near-infrared luminescence detection of singlet oxygen generated by photodynamic therapy in cells in vitro and tissues in vivo. Photochem Photobiol. 2002; 75(4):382–91. [PubMed: 12003128]
20. Jarvi MT, Niedre MJ, Patterson MS, Wilson BC. Singlet oxygen luminescence dosimetry (SOLD) for photodynamic therapy: current status, challenges and future prospects. Photochem Photobiol. 2006; 82(5):1198–210. [PubMed: 16808593]
21. Lee S, Vu DH, Hinds MF, Davis SJ, Liang A, Hasan T. Pulsed diode laser-based singlet oxygen monitor for photodynamic therapy: in vivo studies of tumor-laden rats. J Biomed Opt. 2008; 13(6): 064035. [PubMed: 19123681]
22. Gemmell NR, McCarthy A, Liu B, Tanner MG, Dorenbos SD, Zwiller V, Patterson MS, Buller GS, Wilson BC, Hadfield RH. Singlet oxygen luminescence detection with a fiber-coupled superconducting nanowire single-photon detector. Opt Express. 2013; 21(4):5005–13. [PubMed: 23482033]

23. Wilson BC, Patterson MS. The physics, biophysics and technology of photodynamic therapy. Phys Med Biol. 2008; 53(9):R61–109. [PubMed: 18401068]
24. Nadeau V, O'Dwyer M, Hamdan K, Tait I, Padgett M. In vivo measurement of 5-aminolaevulinic acid-induced protoporphyrin IX photobleaching: a comparison of red and blue light of various intensities. Photodermatol Photoimmunol Photomed. 2004; 20(4):170–4. [PubMed: 15238094]
25. Moan J, Ma L, Iani V, Juzeniene A. Influence of light exposure on the kinetics of protoporphyrin IX formation in normal skin of hairless mice after application of 5-aminolevulinic acid methyl ester. J Invest Dermatol. 2005; 125(5):1039–44. [PubMed: 16297207]
26. Juzenas P, Juzeniene A. Reduction of cutaneous photosensitivity by application of ointment containing ferrous or cobaltous ions concomitant with the use of topical protoporphyrin IX precursors. Photodiagnosis Photodyn Ther. 2010; 7(3):152–7. [PubMed: 20728838]
27. Wagnières GA, Star WM, Wilson BC. In vivo fluorescence spectroscopy and imaging for oncological applications. Photochem Photobiol. 1998; 68(5):603–32. [PubMed: 9825692]
28. Bodaness RS, Heller DF, Krasinski J, King DS. The two-photon laser-induced fluorescence of the tumor-localizing photosensitizer hematoporphyrin derivative. Resonance-enhanced 750 nm two-photon excitation into the near-UV Soret band. J Biol Chem. 1986; 261(26):12098–101. [PubMed: 3745180]
29. Burke TG, Malak H, Gryczynski I, Mi Z, Lakowicz JR. Fluorescence detection of the anticancer drug topotecan in plasma and whole blood by two-photon excitation. Anal Biochem. 1996; 242(2): 266–70. [PubMed: 8937572]
30. Wu J, Feld MS, Rava RP. Analytical model for extracting intrinsic fluorescence in turbid media. Appl Opt. 1993; 32(19):3585–95. [PubMed: 20829983]
31. Ahmed SA, Zang ZW, Yoo KM, Ali MA, Alfano RR. Effect of multiple light scattering and self-absorption on the fluorescence and excitation spectra of dyes in random media. Appl Opt. 1994; 33(13):2746–50. [PubMed: 20885633]
32. Durkin AJ, Jaikumar S, Ramanujam N, Richards-Kortum R. Relation between fluorescence spectra of dilute and turbid samples. Appl Opt. 1994; 33(3):414–23. [PubMed: 20862033]
33. Bradley RS, Thorniley MS. A review of attenuation correction techniques for tissue fluorescence. J R Soc Interface. 2006; 3(6):1–13. [PubMed: 16849213]
34. Gruber JD, Paliwal A, Krishnaswamy V, Ghadyani H, Jermyn M, O'Hara JA, Davis SC, Kerley-Hamilton JS, Shworak NW, Maytin EV, Hasan T, Pogue BW. System development for high frequency ultrasound-guided fluorescence quantification of skin layers. J Biomed Opt. 2010; 15(2):026028. [PubMed: 20459273]
35. Kim A, Khurana M, Moriyama Y, Wilson BC. Quantification of in vivo fluorescence decoupled from the effects of tissue optical properties using fiber-optic spectroscopy measurements. J Biomed Opt. 2010; 15(6):067006. [PubMed: 21198210]
36. Bigio IJ, Mourant JR. Ultraviolet and visible spectroscopies for tissue diagnostics: fluorescence spectroscopy and elastic-scattering spectroscopy. Phys Med Biol. 1997; 42(5):803–14. [PubMed: 9172260]
37. Lim L, Nichols B, Rajaram N, Tunnell JW. Probe pressure effects on human skin diffuse reflectance and fluorescence spectroscopy measurements. J Biomed Opt. 2011; 16(1):011012. [PubMed: 21280899]
38. de Leeuw J, van der Beek N, Neugebauer WD, Bjerring P, Neumann HA. Fluorescence detection and diagnosis of non-melanoma skin cancer at an early stage. Lasers Surg Med. 2009; 41(2):96–103. [PubMed: 19226578]
39. Wang I, Svanberg K, Andersson-Engels S, Berg R, Svanberg S. Photodynamic therapy of non-melanoma skin malignancies with topical δ-amino levulinic acid: diagnostic measurements. Proc SPIE. 1995; 2371:243–52.
40. Johansson J, Berg R, Svanberg K, Svanberg S. Laser-induced fluorescence studies of normal and malignant tumour tissue of rat following intravenous injection of delta-amino levulinic acid. Lasers Surg Med. 1997; 20(3):272–9. [PubMed: 9138256]
41. Peng Q, Moan J, Warloe T, Nesland JM, Rimington C. Distribution and photosensitizing efficiency of porphyrins induced by application of exogenous 5-aminolevulinic acid in mice bearing mammary carcinoma. Int J Cancer. 1992; 52(3):433–43. [PubMed: 1399120]

42. Rhodes LE, Tsoukas MM, Anderson RR, Kollias N. Iontophoretic delivery of ALA provides a quantitative model for ALA pharmacokinetics and PpIX phototoxicity in human skin. J Invest Dermatol. 1997; 108(1):87–91. [PubMed: 8980294]
43. Lesar A, Padgett M, O'Dwyer M, Ferguson J, Moseley H. Fluorescence induced by aminolevulinic acid and methyl aminolevulinate on normal skin. Photodiagnosis Photodyn Ther. 2007; 4(4):224–9. [PubMed: 25047556]
44. Dögnitz N, Salomon D, Zellweger M, Ballini JP, Gabrecht T, Lange N, van den Bergh H, Wagnières G. Comparison of ALA- and ALA hexyl-ester-induced PpIX depth distribution in human skin carcinoma. J Photochem Photobiol B. 2008; 93(3):140–8. [PubMed: 18818091]
45. Di Venosa G, Hermida L, Fukuda H, Defain MV, Rodriguez L, Mamone L, MacRobert A, Casas A, Batlle A. Comparation of liposomal formulations of ALA undecanoyl ester for its use in photodynamic therapy. J Photochem Photobiol B. 2009; 96(2):152–8. [PubMed: 19560367]
46. Bender J, Ericson MB, Merclin N, Iani V, Rosén A, Engström S, Moan J. Lipid cubic phases for improved topical drug delivery in photodynamic therapy. J Control Release. 2005; 106(3):350–60. [PubMed: 15967535]
47. Donnelly RF, Juzenas P, McCarron PA, Ma LW, Woolfson AD, Moan J. Influence of formulation factors on methyl-ALA-induced protoporphyrin IX accumulation in vivo. Photodiagnosis Photodyn Ther. 2006; 3(3):190–201. [PubMed: 25049154]
48. Golub AL, Dickson EFG, Kennedy JC, Marcus SL, Park Y, Pottier RH. The monitoring of ALA-induced protoporphyrin IX accumulation and clearance in patients with skin lesions by in vivo surface-detected fluorescence spectroscopy. Laser Med Sci. 1999; 14(2):112–22.
49. Warren CB, Lohser S, Wene LC, Pogue BW, Bailin PL, Maytin EV. Noninvasive fluorescence monitoring of protoporphyrin IX production and clinical outcomes in actinic keratoses following short-contact application of 5-aminolevulinate. J Biomed Opt. 2010; 15(5):051607. [PubMed: 21054081]
50. Ascencio M, Collinet P, Farine MO, Mordon S. Protoporphyrin IX fluorescence photobleaching is a useful tool to predict the response of rat ovarian cancer following hexaminolevulinate photodynamic therapy. Lasers Surg Med. 2008; 40(5):332–41. [PubMed: 18563777]
51. Heyerdahl H, Wang I, Liu DL, Berg R, Andersson-Engels S, Peng Q, Moan J, Svanberg S, Svanberg K. Pharmacokinetic studies on 5-aminolevulinic acid-induced protoporphyrin IX accumulation in tumours and normal tissues. Cancer Lett. 1997; 112(2):225–31. [PubMed: 9066732]
52. Pye A, Curnow A. Direct comparison of delta-aminolevulinic acid and methyl-aminolevulinate-derived protoporphyrin IX accumulations potentiated by desferrioxamine or the novel hydroxypyridinone iron chelator CP94 in cultured human cells. Photochem Photobiol. 2007; 83(3):766–73. [PubMed: 17576385]
53. Profio AE, Doiron DR, King EG. Laser fluorescence bronchoscope for localization of occult lung tumors. Med Phys. 1979; 6(6):523–5. [PubMed: 545124]
54. Straight RC, Benner RE, McClane RW, Go PM, Yoon G, Dixon JA. Application of charge-coupled device technology for measurement of laser light and fluorescence distribution in tumors for photodynamic therapy. Photochem Photobiol. 1991; 53(6):787–96. [PubMed: 1886937]
55. Tyrrell J, Campbell SM, Curnow A. Monitoring the accumulation and dissipation of the photosensitizer protoporphyrin IX during standard dermatological methyl-aminolevulinate photodynamic therapy utilizing non-invasive fluorescence imaging and quantification. Photodiagnosis Photodyn Ther. 2011; 8(1):30–8. [PubMed: 21333932]
56. van der Beek N, de Leeuw J, Demmendal C, Bjerring P, Neumann HA. PpIX fluorescence combined with auto-fluorescence is more accurate than PpIX fluorescence alone in fluorescence detection of non-melanoma skin cancer: an intra-patient direct comparison study. Lasers Surg Med. 2012; 44(4):271–6. [PubMed: 22170313]
57. Baumgartner R, Fisslinger H, Jocham D, Lenz H, Ruprecht L, Stepp H, Unsöld E. A fluorescence imaging device for endoscopic detection of early stage cancer--instrumental and experimental studies. Photochem Photobiol. 1987; 46(5):759–63. [PubMed: 2964662]
58. Brodbeck KJ, Profio AE, Frewin T, Balchum OJ. A system for real time fluorescence imaging in color for tumor diagnosis. Med Phys. 1987; 14(4):637–9. [PubMed: 2957581]

59. Kohl M, Neukammer J, Sukowski U, Rinneberg HH, Sinn HJ, Friedrich EA, Graschew G, Schlag PM, Woehrle D. Imaging of tumors by time-delayed laser-induced fluorescence. Proc SPIE. 1991; 1525:26–34.10.1117/12.48208
60. Andersson-Engels S, Johansson J, Svanberg K, Svanberg S. Multi-colour fluorescence imaging in connection with photodynamic therapy of deltaaminolevulinic acid (ALA) sensitised skin malignancies. Bioimaging. 1995; 3:134–43.
61. Fischer F, Dickson EF, Pottier RH, Wieland H. An affordable, portable fluorescence imaging device for skin lesion detection using a dual wavelength approach for image contrast enhancement and aminolaevulinic acid-induced protoporphyrin IX. Part I. Design, spectral and spatial characteristics. Lasers Med Sci. 2001; 16(3):199–206. [PubMed: 11482818]
62. Hewett J, Nadeau V, Ferguson J, Moseley H, Ibbotson S, Allen JW, Sibbett W, Padgett M. The application of a compact multispectral imaging system with integrated excitation source to in vivo monitoring of fluorescence during topical photodynamic therapy of superficial skin cancers. Photochem Photobiol. 2001; 73(3):278–82. [PubMed: 11281024]
63. Cuccia DJ, Bevilacqua F, Durkin AJ, Ayers FR, Tromberg BJ. Quantitation and mapping of tissue optical properties using modulated imaging. J Biomed Opt. 2009; 14(2):024012. [PubMed: 19405742]
64. Saager RB, Cuccia DJ, Saggese S, Kelly KM, Durkin AJ. Quantitative fluorescence imaging of protoporphyrin IX through determination of tissue optical properties in the spatial frequency domain. J Biomed Opt. 2011; 16(12):126013. [PubMed: 22191930]
65. Sunar U, Rohrbach DJ, Morgan J, Zeitouni N, Henderson BW. Quantification of PpIX concentration in basal cell carcinoma and squamous cell carcinoma models using spatial frequency domain imaging. Biomed Opt Express. 2013; 4(4):531–7. [PubMed: 23577288]
66. Valdes PA, Leblond F, Kim A, Wilson BC, Paulsen KD, Roberts DW. A spectrally constrained dual-band normalization technique for protoporphyrin IX quantification in fluorescence-guided surgery. Opt Lett. 2012; 37(11):1817–9. [PubMed: 22660039]
67. Lue N, Kang JW, Yu CC, Barman I, Dingari NC, Feld MS, Dasari RR, Fitzmaurice M. Portable optical fiber probe-based spectroscopic scanner for rapid cancer diagnosis: a new tool for intraoperative margin assessment. PLoS One. 2012; 7(1):e30887. [PubMed: 22303465]
68. Rossberger S, Ach T, Best G, Cremer C, Heintzmann R, Dithmar S. High-resolution imaging of autofluorescent particles within drusen using structured illumination microscopy. Br J Ophthalmol. 2013; 97(4):518–23. [PubMed: 23410731]
69. Hoffman ZR, DiMarzio CA. Structured illumination microscopy using random intensity incoherent reflectance. J Biomed Opt. 2013; 18(6):061216. [PubMed: 23183657]
70. Ducros N, Bassi A, Valentini G, Canti G, Arridge S, D'Andrea C. Fluorescence molecular tomography of an animal model using structured light rotating view acquisition. J Biomed Opt. 2013; 18(2):20503. [PubMed: 23344841]
71. Zhu Q, Chen NG, Piao D, Guo P, Ding X. Design of near-infrared imaging probe with the assistance of ultrasound localization. Appl Opt. 2001; 40(19):3288–303. [PubMed: 11958271]
72. Cammarota T, Pinto F, Magliaro A, Sarno A. Current uses of diagnostic high-frequency US in dermatology. Eur J Radiol. 1998; 27(Suppl 2):S215–23. [PubMed: 9652525]
73. Flynn BP, D'Souza AV, Kanick SC, Davis SC, Pogue BW. White light-informed optical properties improve ultrasound-guided fluorescence tomography of photoactive protoporphyrin IX. J Biomed Opt. 2013; 18(4):046008. [PubMed: 23584445]
74. Desai TD, Desai AD, Horowitz DC, Kartono F, Wahl T. The use of high-frequency ultrasound in the evaluation of superficial and nodular basal cell carcinomas. Dermatol Surg. 2007; 33(10): 1220–7. discussion 1226–7. [PubMed: 17903155]
75. Crisan M, Crisan D, Sannino G, Lupsor M, Badea R, Amzica F. Ultrasonographic staging of cutaneous malignant tumors: an ultrasonographic depth index. Arch Dermatol Res. 2013; 305(4): 305–13. [PubMed: 23400334]
76. Huang D, Swanson EA, Lin CP, Schuman JS, Stinson WG, Chang W, Hee MR, Flotte T, Gregory K, Puliafito CA, Fujimoto JG. Optical coherence tomography. Science. 1991; 254(5035):1178–81. [PubMed: 1957169]

77. Gambichler T, Orlikov A, Vasa R, Moussa G, Hoffmann K, Stucker M, Altmeyer P, Bechara FG. In vivo optical coherence tomography of basal cell carcinoma. J Dermatol Sci. 2007; 45(3):167–73. [PubMed: 17215110]

78. Mogensen M, Nurnberg BM, Forman JL, Thomsen JB, Thrane L, Jemec GB. In vivo thickness measurement of basal cell carcinoma and actinic keratosis with optical coherence tomography and 20-MHz ultrasound. Br J Dermatol. 2009; 160(5):1026–33. [PubMed: 19183171]

79. Yun S, Tearney G, Bouma B, Park B, de Boer J. High-speed spectral-domain optical coherence tomography at 1. 3 mum wavelength. Opt Express. 2003; 11(26):3598–604. [PubMed: 19471496]

80. Kepshire DS, Davis SC, Dehghani H, Paulsen KD, Pogue BW. Subsurface diffuse optical tomography can localize absorber and fluorescent objects but recovered image sensitivity is nonlinear with depth. Appl Opt. 2007; 46(10):1669–78. [PubMed: 17356609]

81. Kepshire D, Davis SC, Dehghani H, Paulsen KD, Pogue BW. Fluorescence tomography characterization for sub-surface imaging with protoporphyrin IX. Opt Express. 2008; 16(12): 8581–93. [PubMed: 18545571]

82. Davis SC, Dehghani H, Wang J, Jiang S, Pogue BW, Paulsen KD. Image-guided diffuse optical fluorescence tomography implemented with Laplacian-type regularization. Opt Express. 2007; 15(7):4066–82. [PubMed: 19532650]

83. Boone MA, Norrenberg S, Jemec GB, Del Marmol V. Imaging of basal cell carcinoma by high-definition optical coherence tomography: histomorphological correlation. A pilot study. Br J Dermatol. 2012; 167(4):856–64. [PubMed: 22862425]

84. Maier T, Braun-Falco M, Hinz T, Schmid-Wendtner MH, Ruzicka T, Berking C. Morphology of basal cell carcinoma in high definition optical coherence tomography: en-face and slice imaging mode, and comparison with histology. J Eur Acad Dermatol Venereol. 2013; 27(1):e97–104. [PubMed: 22540280]

85. Selkin B, Rajadhyaksha M, Gonzalez S, Langley RG. In vivo confocal microscopy in dermatology. Dermatol Clin. 2001; 19(2):369–77. ix–x. [PubMed: 11556245]

86. Chung VQ, Dwyer PJ, Nehal KS, Rajadhyaksha M, Menaker GM, Charles C, Jiang SB. Use of ex vivo confocal scanning laser microscopy during Mohs surgery for nonmelanoma skin cancers. Dermatol Surg. 2004; 30(12 Pt 1):1470–8. [PubMed: 15606734]

87. Lademann J, Otberg N, Richter H, Meyer L, Audring H, Teichmann A, Thomas S, Knuttel A, Sterry W. Application of optical non-invasive methods in skin physiology: a comparison of laser scanning microscopy and optical coherent tomography with histological analysis. Skin Res Technol. 2007; 13(2):119–32. [PubMed: 17374052]

88. Astner S, Dietterle S, Otberg N, Rowert-Huber HJ, Stockfleth E, Lademann J. Clinical applicability of in vivo fluorescence confocal microscopy for noninvasive diagnosis and therapeutic monitoring of nonmelanoma skin cancer. J Biomed Opt. 2008; 13(1):014003. [PubMed: 18315361]

89. De Rosa FS, Marchetti JM, Thomazini JA, Tedesco AC, Bentley MV. A vehicle for photodynamic therapy of skin cancer: influence of dimethylsulphoxide on 5-aminolevulinic acid in vitro cutaneous permeation and in vivo protoporphyrin IX accumulation determined by confocal microscopy. J Control Release. 2000; 65(3):359–66. [PubMed: 10699294]

90. Masters BR, So PT, Gratton E. Multiphoton excitation fluorescence microscopy and spectroscopy of in vivo human skin. Biophys J. 1997; 72(6):2405–12. [PubMed: 9168018]

91. König K, Riemann I. High-resolution multiphoton tomography of human skin with subcellular spatial resolution and picosecond time resolution. J Biomed Opt. 2003; 8(3):432–9. [PubMed: 12880349]

92. Schenke-Layland K, Riemann I, Damour O, Stock UA, König K. Two-photon microscopes and in vivo multiphoton tomographs – powerful diagnostic tools for tissue engineering and drug delivery. Adv Drug Deliv Rev. 2006; 58(7):878–96. [PubMed: 17011064]

93. Lin SJ, Jee SH, Dong CY. Multiphoton microscopy: a new paradigm in dermatological imaging. Eur J Dermatol. 2007; 17(5):361–6. [PubMed: 17673377]

94. Becker W, Bergmann A, Biskup C. Multispectral fluorescence lifetime imaging by TCSPC. Microsc Res Tech. 2007; 70(5):403–9. [PubMed: 17393532]

95. Elson D, Requejo-Isidro J, Munro I, Reavell F, Siegel J, Suhling K, Tadrous P, Benninger R, Lanigan P, McGinty J, Talbot C, Treanor B, Webb S, Sandison A, Wallace A, Davis D, Lever J, Neil M, Phillips D, Stamp G, French P. Time-domain fluorescence lifetime imaging applied to biological tissue. Photochem Photobiol Sci. 2004; 3(8):795–801. [PubMed: 15295637]

96. Benati E, Bellini V, Borsari S, Dunsby C, Ferrari C, French P, Guanti M, Guardoli D, Koenig K, Pellacani G, Ponti G, Schianchi S, Talbot C, Seidenari S. Quantitative evaluation of healthy epidermis by means of multiphoton microscopy and fluorescence lifetime imaging microscopy. Skin Res Technol. 201110.1111/j.1600-0846.2011.00496.x

97. Seidenari S, Arginelli F, Dunsby C, French P, König K, Magnoni C, Manfredini M, Talbot C, Ponti G. Multiphoton laser tomography and fluorescence lifetime imaging of basal cell carcinoma: morphologic features for non-invasive diagnostics. Exp Dermatol. 2012; 21(11):831–6. [PubMed: 22882324]

98. Madsen SJ, Sun CH, Tromberg BJ, Wallace VP, Hirschberg H. Photodynamic therapy of human glioma spheroids using 5-aminolevulinic acid. Photochem Photobiol. 2000; 72(1):128–34. [PubMed: 10911737]

99. Lu S, Chen JY, Zhang Y, Ma J, Wang PN, Peng Q. Fluorescence detection of protoporphyrin IX in living cells: a comparative study on single- and two-photon excitation. J Biomed Opt. 2008; 13(2): 024014. [PubMed: 18465977]

100. Goyan RL, Cramb DT. Near-infrared two-photon excitation of protoporphyrin IX: photodynamics and photoproduct generation. Photochem Photobiol. 2000; 72(6):821–7. [PubMed: 11140272]

101. Riemann I, Ehlers A, Dill-Müller D, Martin S, König K. Multiphoton tomography of skin tumors after ALA application. Proc SPIE. 2007; 6424:642405.10.1117/12.702411

102. Cicchi R, Sestini S, De Giorgi V, Massi D, Lotti T, Pavone FS. Nonlinear laser imaging of skin lesions. J Biophotonics. 2008; 1(1):62–73. [PubMed: 19343636]

103. Kantelhardt SR, Diddens H, Leppert J, Rohde V, Hüttmann G, Giese A. Multiphoton excitation fluorescence microscopy of 5-aminolevulinic acid induced fluorescence in experimental gliomas. Lasers Surg Med. 2008; 40(4):273–81. [PubMed: 18412229]

104. Kemmner W, Wan K, Rüttinger S, Ebert B, Macdonald R, Klamm U, Moesta KT. Silencing of human ferrochelatase causes abundant protoporphyrin-IX accumulation in colon cancer. FASEB J. 2008; 22(2):500–9. [PubMed: 17875605]

105. Kantere D, Guldbrand S, Paoli J, Goksör M, Hanstorp D, Wennberg AM, Smedh M, Ericson MB. Anti-Stokes fluorescence from endogenously formed protoporphyrin IX – implications for clinical multiphoton diagnostics. J Biophotonics. 2013; 6(5):409–15. [PubMed: 22997024]

106. Tschen EH, Wong DS, Pariser DM, Dunlap FE, Houlihan A, Ferdon MB. Phase IV ALA-PDT Actinic Keratosis Study Group. Photodynamic therapy using aminolaevulinic acid for patients with nonhyperkeratotic actinic keratoses of the face and scalp: phase IV multicentre clinical trial with 12-month follow up. Br J Dermatol. 2006; 155(6):1262–9. [PubMed: 17107399]

107. Togsverd-Bo K, Haak CS, Thaysen-Petersen D, Wulf HC, Anderson RR, Haedersdal M. Intensified photodynamic therapy of actinic keratoses with fractional CO_2 laser: a randomized clinical trial. Br J Dermatol. 2012; 166(6):1262–9. [PubMed: 22348388]

108. Tyrrell JS, Campbell SM, Curnow A. The relationship between protoporphyrin IX photobleaching during real-time dermatological methyl-aminolevulinate photodynamic therapy (MAL-PDT) and subsequent clinical outcome. Lasers Surg Med. 2010; 42(7):613–9. [PubMed: 20806386]

109. de Bruijn HS, Meijers C, van der Ploeg-van den Heuvel A, Sterenborg HJ, Robinson DJ. Microscopic localisation of protoporphyrin IX in normal mouse skin after topical application of 5-aminolevulinic acid or methyl 5-aminolevulinate. J Photochem Photobiol B. 2008; 92(2):91–7. [PubMed: 18571933]

110. de Haas ER, Kruijt B, Sterenborg HJ, Martino Neumann HA, Robinson DJ. Fractionated illumination significantly improves the response of superficial basal cell carcinoma to aminolevulinic acid photodynamic therapy. J Invest Dermatol. 2006; 126(12):2679–86. [PubMed: 16841035]

111. de Haas ER, de Bruijn HS, Sterenborg HJ, Neumann HA, Robinson DJ. Microscopic distribution of protoporphyrin (PpIX) fluorescence in superficial basal cell carcinoma during light-

fractionated aminolaevulinic acid photodynamic therapy. Acta Derm Venereol. 2008; 88(6):547–54. [PubMed: 19002337]

112. de Vijlder HC, Sterenborg HJ, Neumann HA, Robinson DJ, de Haas ER. Light fractionation significantly improves the response of superficial basal cell carcinoma to aminolaevulinic acid photodynamic therapy: five-year follow-up of a randomized, prospective trial. Acta Derm Venereol. 2012; 92(6):641–7. [PubMed: 22964973]

113. Valentine RM, Ibbotson SH, Wood K, Brown CT. Modelling fluorescence in clinical photodynamic therapy. Photochem Photobiol Sci. 2013; 12(1):203–13. [PubMed: 23128146]

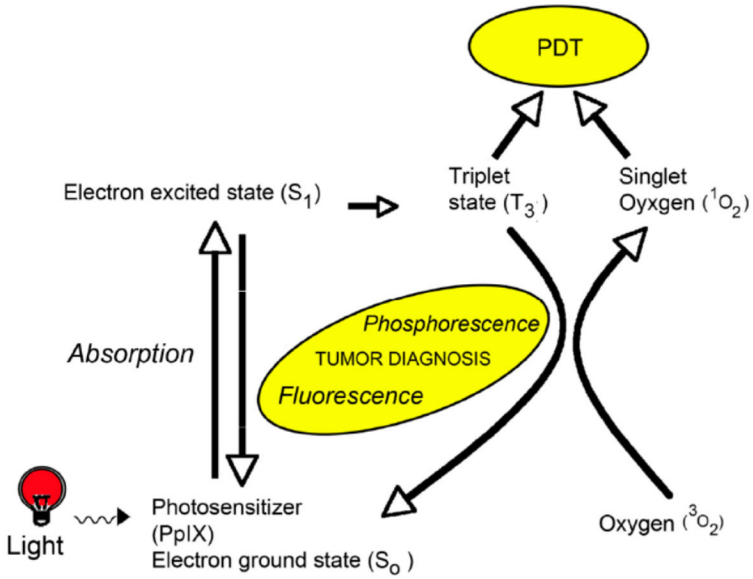

Figure 1.
Schematic diagram of the physical basis of PDT.

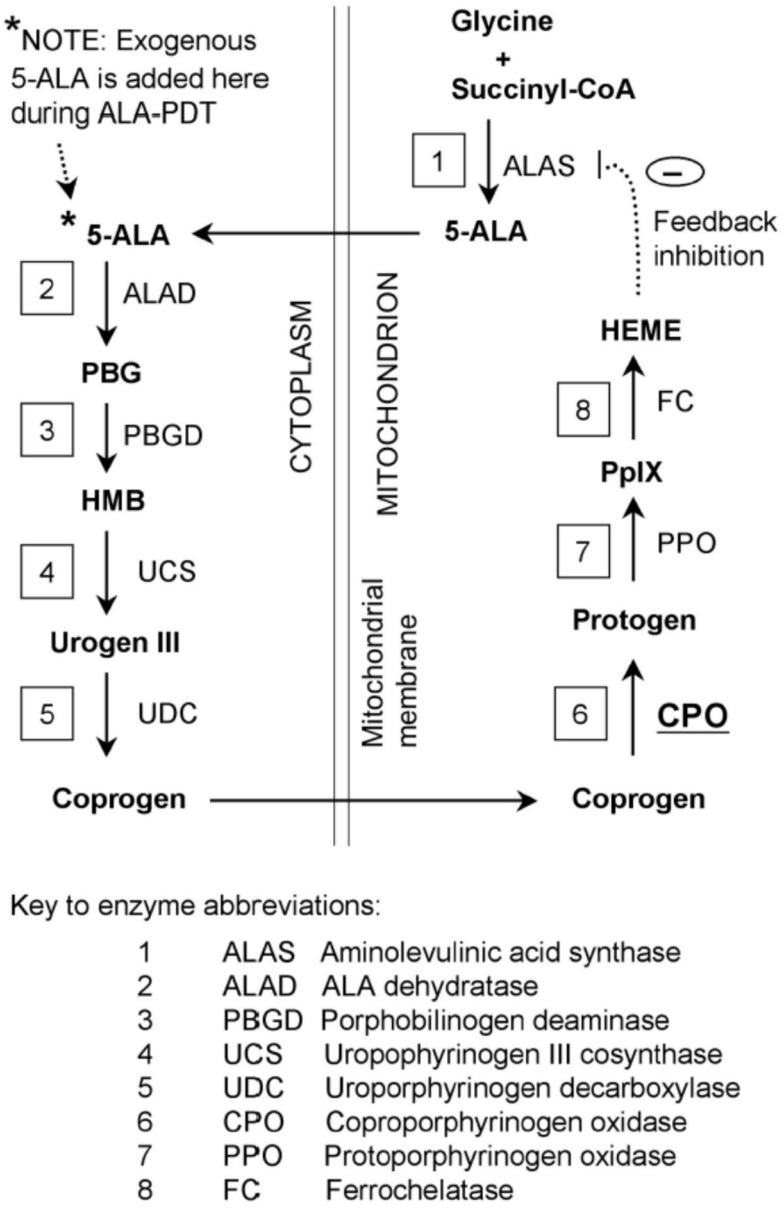

Figure 2.

Schematic of porphyrin-synthetic pathway to illustrate potential control points for increased PpIX accumulation. Enzymes, with names abbreviated and relative locations in the pathway shown in boxes are numbered beginning with the initial condensation of glycine and succinyl-CoA. Substrates/products are shown in bold font. The intracellular location of enzymes, relative to the mitochondria and the cytoplasm, is indicated.

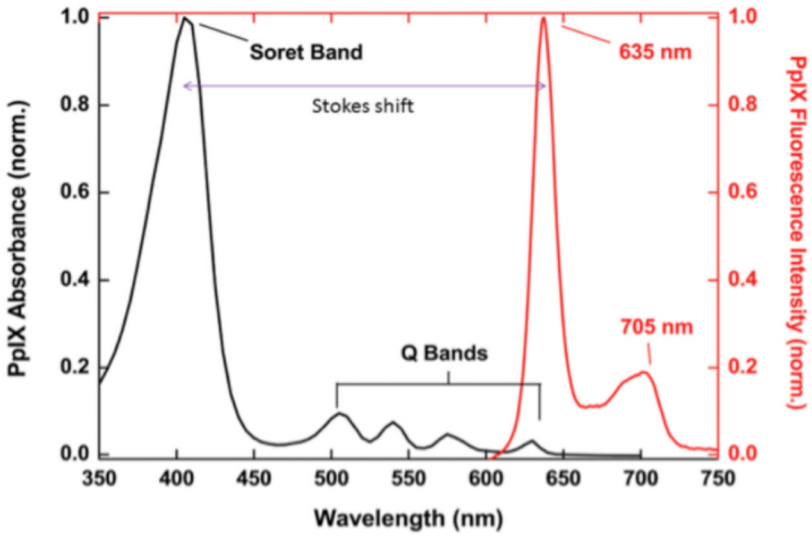

Figure 3.
Absorption and emission spectra of PpIX. (From [113], used with permission.)

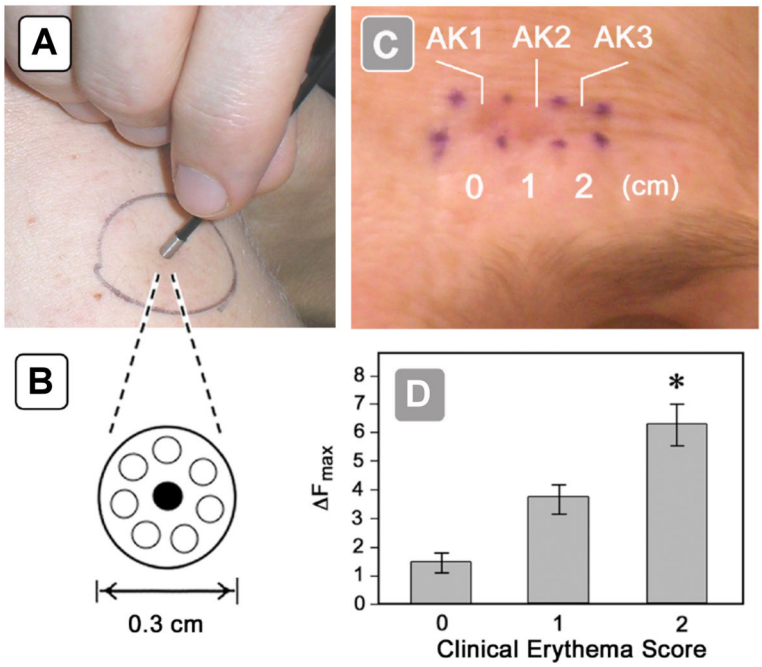

Figure 4.

Clinical use of a non-invasive fluorescence dosimeter for point measurements. (A) Fluorescence probe applied to patient skin during measurement. (B) Close-up of probe tip, viewed end-on. The central optical fiber carries excitation light (405 nm) to the skin, and the peripheral optical fibers carry the fluorescent PpIX emissions back to the detector. (C) Clinical appearance of erythema in 3 actinic keratosis (AK) lesions on a patient's forehead seen immediately after PDT illumination. Erythema for lesions AK1 and AK2 was graded as a score of 2, while for lesion AK3 the erythema is graded as zero. (D) Post-illumination erythema (x-axis) as a function of the PpIX fluorescence (ΔF) measured prior to treatment (y-axis). (From [49], used with permission.)

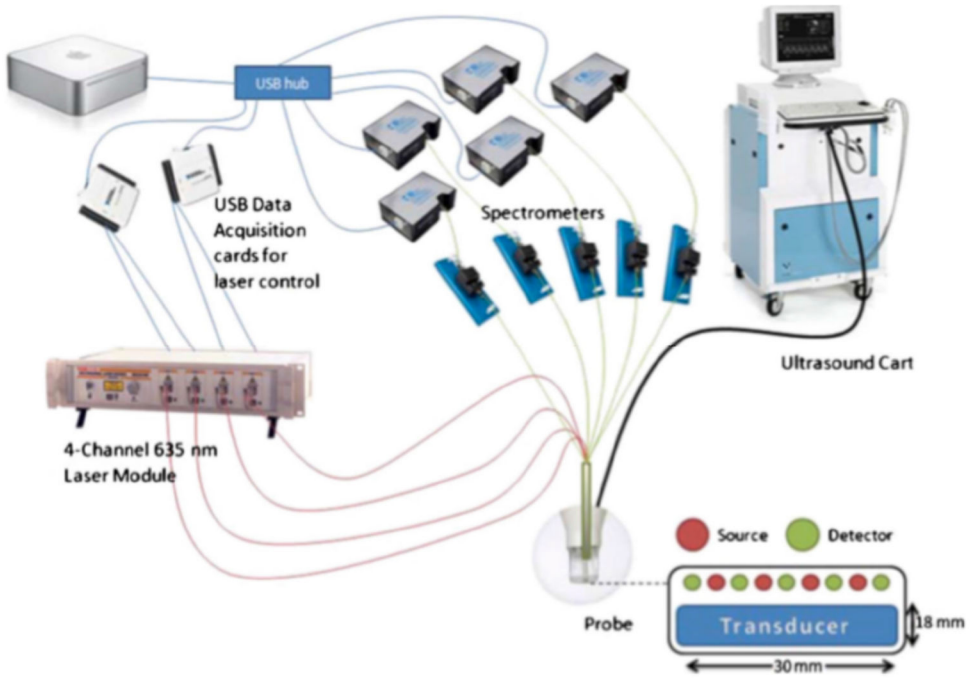

Figure 5.
Schematic representation of the system developed for high frequency ultrasound-guided fluorescence quantification of skin layers. (From [34], used with permission.)

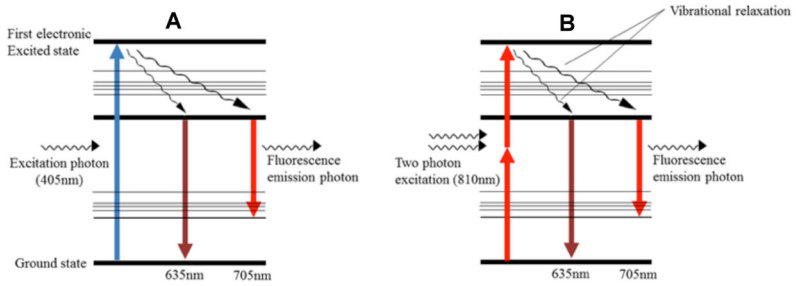

Figure 6.

Jablonski diagrams illustrating one-photon (A) and two-photon (B) excitation for PpIX. Excitation occurs between ground state and the first electronic excited state. After either excitation process, the PpIX molecule relaxes to the lowest excited electronic state level via vibrational processes. The subsequent fluorescence emission is the same for both modes.